JACS
JOURNAL OF THE AMERICAN CHEMICAL SOCIETY

Communication

pubs.acs.org/JACS

Helically Twisted Chiral Arrays of Gold Nanoparticles Coated with a Cholesterol Mesogen

Liliana Cseh,[†] Xiaobin Mang,[§] Xiangbing Zeng,[§] Feng Liu,[§,∥] Georg H. Mehl,*[,†] Goran Ungar,*[,‡,§] and Giuliano Siligardi[⊥]

[†]Department of Chemistry, University of Hull, Hull HU6 7RX, United Kingdom
[‡]Department of Physics, Zhejiang Sci-Tech University, Hangzhou 310018, PR China
[§]Department of Materials Science and Engineering, University of Sheffield, Sheffield S1 3JD, United Kingdom
[∥]State Key Laboratory for Mechanical Behavior of Materials, Xi'an Jiaotong University, Xi'an, 710049, PR China
[⊥]Diamond Light Source, Harwell, Didcot OX11 0DE, United Kingdom

Supporting Information

ABSTRACT: Gold nanoparticles have been prepared and surface-functionalized with a 1:1 molar mixture of a hexylthiol ligand and a chiral mesogenic ligand consisting of a cholesterylbenzoate attached via an undecylthiol spacer. Grazing incidence X-ray diffraction showed that upon annealing a columnar liquid crystal (LC) structure develops with the nanoparticles forming strings on a regular oblique 2*d* lattice. Synchrotron radiation circular dichroism is substantially enhanced upon the isotropic−LC transition. In the proposed structural model, layers of Au columns rotate by a small angle relative to their neighbors, with the columns winding around a helical axis. The work demonstrates that it is possible to obtain chiral LC superstructures from nanoparticles coated with chiral mesogen without the addition of a separate LC or chiral dopants. The results provide direction in the development of plasmonic metamaterials interacting selectively with circularly polarized light.

The breaking of symmetry is one of the most basic tools to introduce functionality into organic materials. In many nematic liquid crystal (LC) display applications, the addition of a small amount of a chiral additive is critical for their performance. The specific optical properties of chiral nematics are also used in nature; striking examples are the chiral nematic photonic structures in the shells of beetles.[1,2] A number of methods have been designed to arrange nanoparticles (NPs) in chiral assemblies.[3−7] The amplification of optical effects by the inclusion of metallic NPs in chiral nematic LCs has recently been explored very actively, especially because the chiral organization of Au or Ag NPs promises fascinating metamaterial behavior.[8−11] Optical metamaterials capable of interacting with circularly polarized (CP) light, based on helical structures, are of considerable interest because CP light can be used in optical communications between spin-LEDs,[12] in displays,[13] or in quantum-based optical computing.[14] So far, efforts to obtain chiral nematics filled with NPs have relied on either adding hydrocarbon-group-capped NPs to a chiral nematic matrix or functionalizing Au NPs with chiral groups and dispersing them in a nematic liquid crystal.[15−22] Mostly, it has been found that NPs aggregate in the defects of the LC texture. This is possibly mediated by the pinning of features of defects such as fingerprint or schlieren textures to surfaces, providing a means of spatial NP assembly. However, this method requires very careful control of the NP concentration in order to avoid phase separation and precipitation. To the best of our knowledge, there have been so far no reported investigations of functionalized NPs forming a chiral LC phase. We note that to achieve significant plasmonic effects which could potentially lead to useful photonic metamaterials a relatively high density of metallic NPs is required that is unlikely to be obtainable by NP doping of LCs.[10,16]

We report here the synthesis and investigation of the phase behavior of a LC−NP system that is intrinsically chiral. Cholesterol-based mesogens are attached to the surface of Au NPs via alkylthiol spacers. The formation of an ordered superlattice is studied by a combination of X-ray diffraction and circular dichroism (CD) using mainly synchrotron radiation. (SRCD denotes experiments using synchrotron light source.) We propose a structural model that is based on an oblique columnar phase made up of strings of Au NPs with each layer of columns slightly twisted relative the neighboring layers. We believe that the result reported herein will help create plasmonic metamaterials selectively interacting with circularly polarized light.

The synthesis and chemical characterization of cholesterol-based thiol ligand **1** is described in the Supporting Information. The synthesis of LC-functionalized Au NPs follows essentially the route described earlier.[23,24] Hexylthiol NPs are synthesized according to a Brust−Schiffrin approach, and an exchange reaction introduced a cholesteryl group attached end-on to a thioalkyl chain (Chart 1, mesogenic unit). Following purification using size-exclusion chromatogaphy over biobeads, Au NPs coated with a 1:1 mixture of *n*-hexylthiol and mesogens **1** were obtained, denoted **AuCholC6**.

From thermogravimetric scanning (Figure S3), we found the weight fraction of Au in **AuCholC6** to be 39%. From elemental analysis, we found the molar fractions of hexylthiol and mesogenic ligands to be 47 and 53%, respectively, of the

Received: May 15, 2015
Published: September 25, 2015

DOI: 10.1021/jacs.5b05059
J. Am. Chem. Soc. 2015, 137, 12736−12739

Chart 1. Sketch of Functionalized Gold Nanoparticle AuCholC6[a]

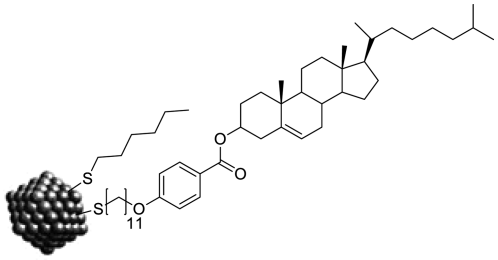

[a]Total number of organic ligands = 78 ± 5, of which 37± 5 are cholesteryl-based mesogens.

organic coating of the NPs (Supporting Information, Section 1.4). This ratio was also confirmed by NMR. TEM of **AuCholC6** precipitated from dilute solution is shown in Figure 1a; the average particle diameter is 1.7 ± 0.4 nm. On the basis of these data, we obtain the average number of Au atoms per particle (151), and a total number of ligands per particle (78 ± 5), of which 37 ± 5 are mesogens. This is in accord with earlier work[25,26] and supported by recent results measuring ligand densities of up to ~6.3 ligands/nm^2. Together with a surface area of the NPs (estimated to be 11.5 to 13 nm^2),[25] this gives 73−82 ligands per particle.[27]

On the basis of DSC and polarized optical microscopy (POM), the phase sequences obtained for **1** and **AuCholC6** are listed in Table 1. Polarized optical micrographs of the chiral nematic (cholesteric) phase N* and the twist grain boundary (TGB) phase of **1** are shown in Figure S4, and X-ray patterns are shown in Figure S7.

Powder small-angle X-ray scattering (SAXS) on annealed **AuCholC6** revealed a mesophase (X in Table 1) with long-range positional order, stable up to 90 °C (Figures 1b and S6). Grazing incidence small-angle X-ray scattering (GISAXS) experiments were also carried out on thin films to obtain oriented samples that helped index the Bragg reflections. For this purpose, a film was melt-cast on silicon substrate and then cooled from 130 to 30 °C at 0.2 °C/min under vacuum. The Bragg spacings in the GISAXS pattern (Figure 1d) match well those in the powder pattern. (See also comment on the diffuse scatter in section 4 of the Supporting Information.) The Bragg reflections were indexed on an oblique 2D lattice (Figure 1d) with unit cell parameters a = 4.54 nm and b = 5.28 nm and the angle γ = 57.0°. The measured and calculated d spacings and diffraction intensities are given in Table S1.

The position of the diffuse maximum next to (10) observed in the powder pattern corresponds to a d spacing of 3.7 nm if Bragg equation were used. However, in dense, disordered particle systems, the correlation function maximum is usually asymmetric,[28] and as a guide, ~10% should be added to the "Bragg" value when estimating the average particle distance, giving a value of ~4.1 nm. This is likely to correspond to the average Au NP distance along the columns.

An electron density (ED) map of the columnar mesophase was reconstructed using the diffraction intensities from the powder pattern in Figure 1b. (See also Figure S9 and numerical data in Table S1.) The ED map (Figure 1c) is a projection of the 3D map onto the xy plane. The purple-blue high-ED regions are the projections of the Au NP strings, surrounded by the low-density organic ligands. This map is unusual compared to those obtained previously in systems where the NPs were coated with

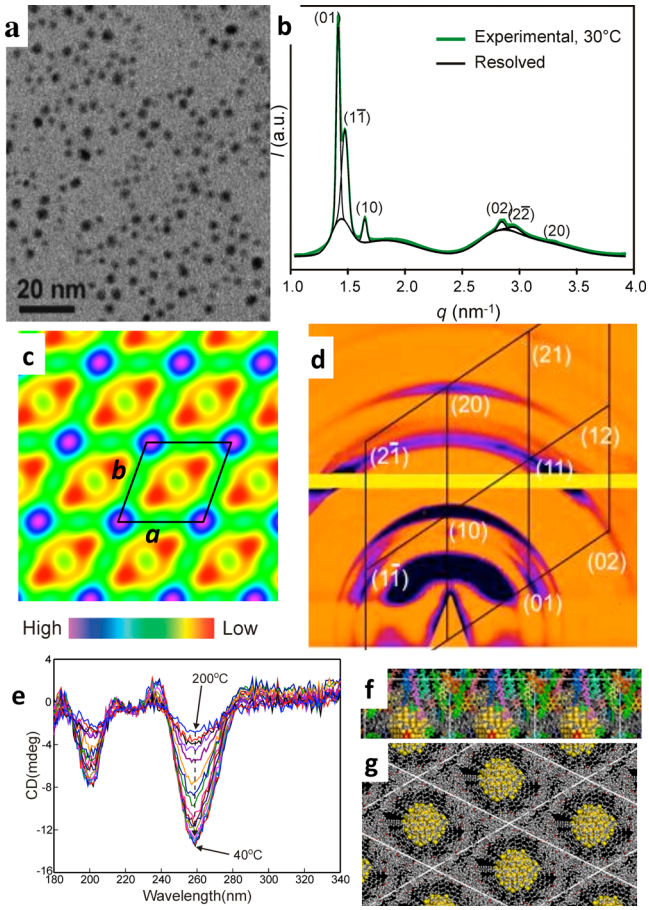

Figure 1. (a) TEM picture of **AuCholC6** on carbon surface. (b) Powder SAXS curve of annealed **AuCholC6** recorded at 30 °C; resolved components are superimposed and indexed. (c) ED map perpendicular to the columns based on intensities of the six reflections in b; all phase angles are zero. (d) GISAXS pattern of a slowly cooled thin film of **AuCholC6** in the mesophase; the reciprocal net is superimposed giving the Miller indices. (e) SRCD spectra of a thin film of **AuCholC6** recorded every 10 °C upon cooling from the isotropic liquid (200 °C) to 40 °C; note the largest increase in ellipticity between 160 and 150 °C, coinciding with the isotropic−columnar transition observed by X-ray diffraction (Figure S17). (f and g) Side and top views, respectively, of a model of several unit cells of **AuCholC6** after molecular dynamics annealing, with unit cell parameters as determined by experiment; in f, each mesogen is colored differently for clarity.

Table 1. Transition Temperatures Determined by DSC[a]

compound	T_t (°C)
1	Cr 114.2 TGB 132.61 N* 186.3 Iso (Figure S4)
AuCholC6	Cr 58.2 X 160 Iso and slow dec

[a]N*= chiral nematic, SmA* = chiral smectic A, X = unknown mesophase (twisted oblique columnar LC, as determined from GISAXS and CD/SRCD, see below); Iso = isotropic liquid.

nonchiral mesogens[29−31] in that the columnar phase is oblique rather than hexagonal or rectangular (see below).

Table S2 details the calculation of the average Au NP diameter on the basis of the above unit cell parameters, the Au weight fraction from TGA, and the assumption that there is one NP per unit cell. The Au NP diameter obtained is 1.69 nm, in excellent somewhat coincidental agreement with the value of 1.7 nm obtained from TEM.

DOI: 10.1021/jacs.5b05059
J. Am. Chem. Soc. 2015, 137, 12736−12739

To establish whether there is helical order in the mesophase of **AuCholC6**, we recorded CD spectra as a function of temperature. If the mesophase contained a helical twist, then an enhancement of the CD signal would occur upon the isotropic−mesophase transition. Fortunately, the LC domains were very small and numerous (Figure S5), causing most of the interfering ellipticity due to linear dichroism and birefringence within the illuminated area to cancel.[32,33] That these interfering effects were indeed negligible was ascertained by rotating the sample during the recording; angular dependence of CD spectrum of **AuCholC6** is shown in Figure S16. Sample rotation, *xy* scanning, recording at high temperatures, and prevention of gravity-induced flow were all made possible by the use of the bright, vertically deflected light beam of synchrotron radiation (Figure S15) only available at module A of B23 beamline.[34] The temperature series of SRCD spectra is shown in Figure 1e. The increasing CD in the UV bands at 200 and 260 nm with lowering temperature is clearly evident. The largest jump is seen between 160 and 150 °C, i.e. at the isotropic−mesophase transition temperature. The temperature-dependent intensity of the 260 nm CD band is plotted in Figure S17, showing typical weak first-order phase transition features. This behavior together with the fact that for the film the CD at about 260 nm (Figure 1e) has a sign opposite of that in solution (Figure S20) is a strong indication of the existence of helical twist in the mesophase superstructure.

The question to be addressed is how is it possible to reconcile a helical twist with a 2D-ordered columnar LC structure? There have been numerous reported examples of intracolumnar helical order in thermotropic[35−37] columnar systems (e.g., ref 38). However, these examples have all involved "classical" column-forming mesogens, typically disclike or wedgelike with spread-out flexible tails forming a shield around each column. In contrast, the ligand in **AuCholC6** is a typical nematogen, albeit chiral, with a tendency to align nearly parallel to its neighbors and form a cholesteric phase. Furthermore, the fact that the 2D lattice is oblique does not support intracolumnar helical structure. Instead, we propose a model that is based on the cholesteric arrangement of the mesogens but with strings of Au NPs threaded through it (Figure 2). In this model, the layers of Au columns rotate by a small angle relative to their neighbors, with the columns winding around the vertical axis forming a helix. Because the POM textures where too fine and did not show a discernible fingerprint pattern characteristic of the cholesteric LC phase, we could not determine the pitch of the helix. No selective reflection of light was observed; hence, the pitch is likely to be outside the visible light wavelengths. The departure from hexagonal symmetry is consistent with this model. Notably, as expected, the twist plane (horizontal in Figure 1c) is the most densely packed plane with the shortest intercolumnar distance within the plane.

In Figure 2, the cholesterol mesogens are drawn with their axis broadly parallel to the NP columns, as has been observed for other rod-shaped mesogens attached to NPs,[28,29] an arrangement driven by the nematogenic tendency of the cholesteryl benzoate and mediated by the long flexible spacer. The structure is supported by molecular modeling (Figures 1f,g). (See also Figures S12 and S13, the former showing an energy-minimized conformation of the mesogenic ligand.) The number of Au atoms and mesogenic ligands per cell are also as determined by experiment (see above). The alternative models in which the cholesteric mesogens would lie preferentially in planes perpendicular to NP column axis would require a larger intercolumnar distance (larger cell cross-section) and a considerably smaller intracolumnar NP spacing and hence are judged less likely. Additional support for the model is presented in section 3 of the Supporting Information.

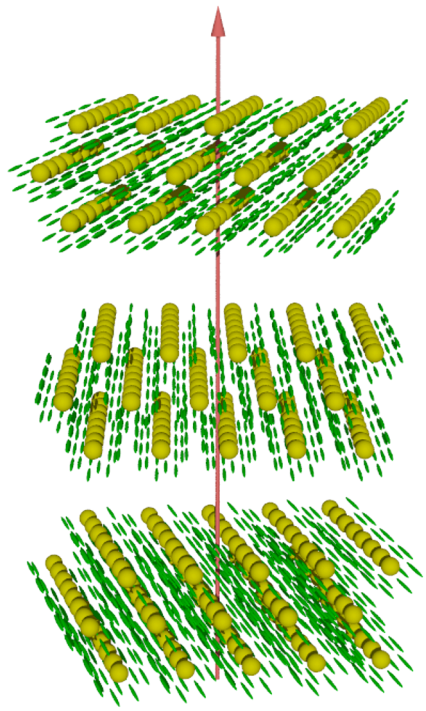

Figure 2. Schematic representation of the chiral columnar LC phase of **AuCholC6**. Yellow: Au NPs, green: mesogenic cholesteryl ligands. The breaks in the stacks of columnar layers indicate that the helical pitch is long on the molecular scale.

It is stressed that the sketch in Figure 2 does not imply a discontinuous twist and that the breaks are meant only to illustrate the presumed large size of the helical pitch compared to the molecular scale.

We have demonstrated that it is possible to obtain chiral LC superstructures from undiluted NPs coated with chiral mesogens. The high NP content achievable in this way should allow the production of plasmonic metamaterials interacting selectively with CP light, extending the range of potential optical applications of LC−NP systems. In future work we will attempt to include mesogens with stronger chirality in order to shorten the helical pitch and to increase the NP size in order to enhance the plasmonic response.

■ ASSOCIATED CONTENT

Supporting Information

The Supporting Information is available free of charge on the ACS Publications website at DOI: 10.1021/jacs.5b05059.

Synthesis and chemical characterization, instrumental methods, optical microscopy, additional X-ray diffraction data, molecular models, UV/vis and CD/SRCD spectra. (PDF)

■ AUTHOR INFORMATION

Corresponding Authors

*g.h.mehl@hull.ac.uk

*g.ungar@sheffield.ac.uk

DOI: 10.1021/jacs.5b05059
J. Am. Chem. Soc. 2015, 137, 12736−12739

Present Address
L.C.: Institute of Chemistry Timisoara of Romanian Academy, Timisoara 300223, Romania; lili_cseh@yahoo.com.

Notes
The authors declare no competing financial interest.

■ ACKNOWLEDGMENTS

For help with X-ray and CD synchrotron experiments we thank Drs. G. Nisbet and Prof. S. Collins of beamline I16, Prof. N. Terrill of I22 and Dr. Tamas Javorfi of B23 at Diamond Light Source. Financial support is acknowledged for the joint NSF-EPSRC PIRE project "RENEW" (EPSRC EP/K034308), the Leverhulme Foundation (RPG-2012−804), for GU the "1000 Talents" program of the Government of China and for LC through the EPSRC project EP/D058066 and the EU FP7 project 228455 "Nanogold".

■ REFERENCES

(1) Neville, A. C.; Caveney, S. *Biol. Rev.* **1969**, *44*, 531.
(2) Sharma, V.; Crne, M.; Park, J. O.; Srinivasarao, M. *Science* **2009**, *325*, 449.
(3) Pendry, P. B. *Science* **2004**, *306*, 1353.
(4) Valev, V. K.; Baumberg, J. J.; Sibilia, C.; Verbiest, T. *Adv. Mater.* **2013**, *25*, 2517.
(5) Rodrigues, S. P.; Lan, S.; Kang, L.; Cui, Y.; Cai, W. *Adv. Mater.* **2014**, *26*, 6157.
(6) Xia, Y.; Zhou, Y.; Tang, Z. *Nanoscale* **2011**, *3*, 1374.
(7) Ma, W.; Kuang, H.; Wang, L.; Xu, L.; Chang, W. S.; Zhang, H.; Sun, M.; Zhu, Y.; Zhao, Y.; Liu, L.; Xu, C.; Link, S.; Kotov, N. A. *Sci. Rep.* **2013**, *3*, 1934.
(8) Lilly, G. D.; Agarwal, A.; Srivastava, S.; Kotov, A. N. *Small* **2011**, *7*, 2004.
(9) Bierman, M. J.; Lau, Y. K. A.; Kvit, A. V.; Schmitt, A. L.; Jin, S. *Science* **2008**, *320*, 1060.
(10) Rockstuhl, C.; Lederer, F.; Etrich, C.; Pertsch, T.; Scharf, T. *Phys. Rev. Lett.* **2007**, *99*, 017401.
(11) Gautier, C.; Bürgi, T. *J. Am. Chem. Soc.* **2006**, *128*, 11079.
(12) Farshchi, R.; Ramsteiner, M.; Herfort, J.; Tahraoui, A.; Grahn, H. T. *Appl. Phys. Lett.* **2011**, *98*, 162508.
(13) Singh, R.; Narayanan Unni, K. N.; Solanki, A.; Deepak, A. *Opt. Mater.* **2012**, *34*, 716.
(14) Sherson, J. F.; Krauter, H.; Olsson, R. K.; Julsgaard, B.; Hammerer, K.; Cirac, I.; Polzik, E. S. *Nature* **2006**, *443*, 557.
(15) Mitov, M.; Portet, C.; Bourgerette, C.; Snoeck, E.; Verelst, M. *Nat. Mater.* **2002**, *1*, 229.
(16) Mitov, M.; Bourgerette, C.; de Guerville, F. *J. Phys.: Condens. Matter* **2004**, *16*, S1981.
(17) Qi, H.; O'Neil, J.; Hegmann, T. *J. Mater. Chem.* **2008**, *18*, 374.
(18) Qi, H.; Hegmann, T. *J. Am. Chem. Soc.* **2008**, *130*, 14201.
(19) Ayeb, H.; Grand, J.; Sellame, S.; Truong, S.; Aubard, J.; Felidj, N.; Mlayah, A.; Lacaze, E. *J. Mater. Chem.* **2012**, *22*, 7856.
(20) Sharma, A.; Mori, T.; Lee, H.-C.; Worden, M.; Bidwell, E.; Hegmann, T. *ACS Nano* **2014**, *8*, 11966.
(21) Pendery, J. S.; Merchiers, O.; Coursault, D.; Grand, J.; Ayeb, H.; Greget, R.; Donnio, B.; Gallani, J. L.; Rosenblatt, C.; Felidj, N.; Borensztein, Y.; Lacaze, E. *Soft Matter* **2013**, *9*, 9366.
(22) Choudhary, A.; Singh, G.; Biradar, A.M. *Nanoscale* **2014**, *6*, 7743.
(23) Cseh, L.; Mehl, G. H. *J. Am. Chem. Soc.* **2006**, *128*, 13376.
(24) Dintinger, J.; Tang, B. J.; Zeng, X.; Liu, F.; Kienzler, T.; Mehl, G. H.; Ungar, G.; Rockstuhl, C.; Scharf, T. *Adv. Mater.* **2013**, *25*, 1999.
(25) Hostetler, M. J.; Wingate, J. E.; Zhong, C.-J.; Harris, J. E.; Vachet, R. W.; Clark, M. R.; Londono, J. D.; Green, S. J.; Stokes, J. J.; Wignall, G. D.; Glish, G. L.; Porter, M. D.; Evans, N. D.; Murray, R. W. *Langmuir* **1998**, *14*, 17−30.
(26) Labande, A.; Ruiz, J.; Astruc, D. *J. Am. Chem. Soc.* **2002**, *124*, 1782−1789. Daniel, M. C.; Ruiz, J.; Nlate, S.; Blais, J. C.; Astruc, D. *J. Am. Chem. Soc.* **2003**, *125*, 2617−2628.
(27) Hinterwirth, H.; Kappel, S.; Waitz, T.; Prohaska, T.; Lindner, W.; Lämmerhoefer, M. *ACS Nano* **2013**, *7*, 1129−1136.
(28) Schulz, G. V. *Z. Phys. Chem., Abt. B* **1939**, *43*, 25.
(29) Zeng, X. B.; Liu, F.; Fowler, A. G.; Ungar, G.; Cseh, L.; Mehl, G. H.; Macdonald, J. E. *Adv. Mater.* **2009**, *21*, 1746.
(30) Mang, X.; Zeng, X. B.; Tang, B.; Liu, F.; Ungar, G.; Zhang, R.; Cseh, L.; Mehl, G. H. *J. Mater. Chem.* **2012**, *22*, 11101.
(31) Kanie, K.; Matsubara, M.; Zeng, X. B.; Liu, F.; Ungar, G.; Nakamura, H.; Muramatsu, A. *J. Am. Chem. Soc.* **2012**, *134*, 808.
(32) Gottarelli, G.; Lena, S.; Masiero, S.; Pieraccini, S.; Spada, G. P. *Chirality* **2008**, *20*, 471.
(33) Otani, T.; Araoka, F.; Ishikawa, K.; Takezoe, H. *J. Am. Chem. Soc.* **2009**, *131*, 12368.
(34) Siligardi, G.; Hussain, R. In *Structural Proteomics: High-Throughput Methods*; Owens, R. J, Ed.; Methods in Molecular Biology Series, Vol. *1261*; Springer: New York, 2015; pp 255−276.
(35) Fontes, E.; Heiney, P. A.; de Jeu, W. H. *Phys. Rev. Lett.* **1988**, *61*, 1202.
(36) Malthête, J.; Collet, A. *J. Am. Chem. Soc.* **1987**, *109*, 7544.
(37) Shcherbina, M. A.; Zeng, X. B.; Tadjiev, T.; Ungar, G.; Eichhorn, S. H.; Phillips, K. E. S.; Katz, T. J. *Angew. Chem., Int. Ed.* **2009**, *48*, 7837.
(38) Vera, F.; Luis Serrano, J.; Sierra, T. *Chem. Soc. Rev.* **2009**, *38*, 781.

DOI: 10.1021/jacs.5b05059
J. Am. Chem. Soc. 2015, 137, 12736−12739